HHS Public Access

Author manuscript

Small. Author manuscript; available in PMC 2017 August 01.

Published in final edited form as:

Small. 2016 August ; 12(32): 4404–4411. doi:10.1002/smll.201600291.

Lanthanide Hydroxide Nanoparticles Induce Angiogenesis *via* ROS-sensitive Signaling

Haishan Zhao[1,2], **Olivia J. Osborne**[3], **Sijie Lin**[4], **Zhaoxia Ji**[3], **Robert Damoiseux**[3], **Yuqiang Wang**[1], **André E. Nel**[3], and **Shuo Lin**[2,3]

[1]College of Pharmacy, Jinan University, Guangzhou, Guangdong, China

[2]Department of Molecular, Cell and Developmental Biology, University of California Los Angeles, Los Angeles, CA

[3]Center for Environmental Implications of Nanotechnology, California NanoSystems Institute, University of California Los Angeles, Los Angeles, CA

[4]College of Environmental Science and Engineering, Tongji University, Shanghai, China

Abstract

Recent studies suggest that the nanorods consisting of europium hydroxide could promote angiogenesis. In this study, we sought to determine if additional types of nanoparticles were capable of enhancing angiogenesis and in addition, understand the underlying mechanisms. For this reason, we employed a method that combines a high throughput *in vitro* cell based screen coupled with an *in vivo* validation using vascular specific green fluorescent protein (GFP) reporter transgenic zebrafish for examining proangiogenesis activity. After screening multiple types of nanoparticles, we discovered that four of them: $Eu^{III}(OH)_3$ rods (Eu Rods), $Eu^{III}(OH)_3$ spheres (Eu Spheres), $Tb^{III}(OH)_3$ rods (Tb Rods) and $Tb^{III}(OH)_3$ spheres (Tb Spheres), were the most effective in promoting angiogenesis. We also showed that ionic forms of europium nitrate [$Eu(NO_3)_3$] (Eu) and terbium nitrate [$Tb(NO_3)_3$] (Tb), the two lanthanide elements for these four nanoparticles, were also capable of enhancing angiogenesis. However, this effect was further enhanced by nanoparticle synthesis. Finally, we demonstrated that reactive oxygen species H_2O_2 is a key factor in the process of proangiogenesis by lanthanide elemental nanoparticles.

Keywords

Reactive oxygen species; Angiogenesis; Zebrafish; Lanthanide Nanoparticles

Introduction

Damage of blood vessels causes ischemia [1]. Cardiac ischemia and peripheral arterial diseases are the two major forms of ischemic diseases and remain top of the list of human health problems [2–4]. One of the treatment options for ischemic diseases is to develop effective agents that can be used *in vivo* to enhance angiogenesis [5], the process of forming new blood vessels from existing vessels through sprouting and branching. In the past, small molecules and recombinant growth factors such as VEGF and FGF have been considered as the choice of agents for therapeutics purposes. Recently, several nanoparticles were

identified as new proangiogenesis agents, which may have better potential to be developed as medicine due to their stability and effectiveness. Specifically, rod-shaped europium hydroxide [$Eu^{III}(OH)_3$] nanoparticles were found to promote angiogenesis by reactive oxygen species (ROS) generated through the Fenton reaction [6, 7].

ROS are a series of molecules derived from oxygen metabolism, such as superoxide anion radical (•$O^{-}2$), hydrogen peroxide (H_2O_2) and ozone (O_3)[8]. Traditionally, ROS are considered byproducts of metabolism, and the increased oxidative stress by ROS would cause damage to different tissues through free-radical mediated chemical chain reactions [9]. However, there is increasing evidence showing that a physiologically appropriate concentration of ROS plays regulatory roles in cell signaling, and is therefore involved in regulating different developmental processes, including angiogenesis [10, 11]. Studies have suggested that ROS affects angiogenesis *via* a regulated activation of some key vascular factors such as VEGF and HIF-1α [12–14]. For example, increasing ROS would inactivate the protein tyrosine phosphatase, which in turn prolongs phosphorylation of activated VEGFR to promote angiogenesis [15, 16].

Considering that there are a variety of nanoparticles, of different sizes and shapes, the possibilities are infinitely limitless; therefore, a more efficient approach to identify pro-angiogenetic candidates from a larger number of nanomaterials would be highly desirable. Towards this aim, we designed a high throughput approach (Fig 1), which uses differentiation of embryonic primary cells to endothelial cells as an initial pre-screen, followed by an *in vivo* validation using the transgenic line Tg (flk:EGFP) zebrafish embryos that have their vascular structure pre-inhibited by a VEGF receptor inhibitor [17, 18]. Based on this approach, we expanded the studies of nanoparticle-enhanced angiogenesis to further investigate the following three related issues: (1) Do other types of nanoparticles have the ability to improve angiogenesis? (2) Can ionic forms of chemical elements that are used to synthesize nanoparticles directly enhance angiogenesis? (3) Is the ROS pathway required to mediate the nanoparticles' ability to enhance angiogenesis? Collectively, we found that lanthanide nanoparticles enhanced angiogenesis through production reactive oxygen species H_2O_2, which is likely a unique attribute conferred by synthesis of nanostructures.

Results

Hydrothermal Synthesis of $Eu^{III}(OH)_3$ and $Tb^{III}(OH)_3$ Nanospheres and Nanorods

Transmission Electron Microscopy (TEM) images of $Eu^{III}(OH)_3$ and Tb $^{III}(OH)_3$ nanoparticles are shown in Fig 2. In the absence of citric acid, $Eu^{III}(OH)_3$ and $Tb^{III}(OH)_3$ particles are in rod shape with diameters of 36±4 nm and 111±18 nm, lengths of 215±29 nm and 847±165 nm, respectively. Once a small amount of citric acid was added to the synthesis system, $Eu^{III}(OH)_3$ and $Tb^{III}(OH)_3$ nanospheres of 21±3 nm and 106±19 nm were formed instead (Table S1). We also performed X-ray diffraction (XRD) analysis and confirmed that all samples were highly crystalline with narrow sharp peaks (Fig S1).

Spherical and rod-shaped $Eu^{III}(OH)_3$ and $Tb^{III}(OH)_3$ nanoparticles improve angiogenesis *in vitro*

In order to examine the angiogenesis potential of nanoparticles with different compositions and shapes, we first used Tg(flk:EGFP) zebrafish embryonic primary cell culture to perform *in vitro* high throughput screening as previously described [17]. This strategy uses genetically stable, endothelial cell-specific GFP transgenic zebrafish embryos at the blastula/gastrula stages to generate pluripotent primary cells, and allows them to differentiate with different nanoparticles *in vitro* [17]. This culture system can be scaled up to screen thousands of nanoparticles for effects on GFP-expressing cells, which are indicative of endothelial differentiation. High content fluorescent images were captured at 4 days after incubation with nanoparticles and the images were subsequently analyzed both manually and automatically by MetaXpress software. As shown in Fig 3, the green signals (both lines and dots) represent the GFP+ endothelial cells differentiated from zebrafish embryonic cells. Screening results of the different nanoparticles showed that individual treatment of Eu Rods, Eu Spheres, Tb Rods or Tb Spheres significantly increased the GFP+ endothelia cells compared to blank controls (Table S2). The angiogenesis growth factor VEGF was used as a positive control for comparison, which showed the highest pro-angiogenesis activity among all treatment groups. Statistical analysis of images revealed that the four lanthanide based nanoparticles enhanced GFP+ cells by a ~1.2 fold increase whereas the VEGF control had a ~1.3 folds increase.

To confirm the proangiogenesis effect determined by automated high content screening and computation analysis, we also performed manual imaging analysis of primary cell culture using a fluorescent microscope. The fluorescence intensity of collected images was analyzed using Photoshop software. The data showed that both methods were capable of detecting proangiogenesis activity (Fig 3 and Fig S2). Both methods are statistically reliable to detect the difference of the fluorescence expressed by endothelial cells, but the manual method seems more sensitive. This difference is likely caused by how background fluorescence is included by the two methods. The automatic method collects data from the entire field of individual wells of 96 well plates, which includes more background fluorescence. The manual method collects data from a section of the field by outlining and tracing individual endothelial cells, which have less background fluorescence. Although the manual method is more labor intensive and time-consuming, it can be an excellent alternative to a low throughput approach. Overall, quantitative analysis of multiple datasets revealed that Tb Spheres had a weaker ability to promote angiogenesis compared to Eu Rods, Eu Spheres and Tb Rods.

Spherical and rod-shaped $[Eu^{III}(OH)_3]$ and $[Tb^{III}(OH)_3]$ nanoparticles improve angiogenesis *in vivo*

After demonstrating that the four forms of europium and terbium hydroxide nanoparticles could promote angiogenesis *in vitro*, we conducted further studies to investigate their proangiogenesis activity *in vivo*, using the transgenic line Tg(flk:EGFP) zebrafish live embryos. In our study, we first treated Tg(flk:EGFP) zebrafish embryos with VEGFR tyrosine kinase inhibitor II (VRI) to prepare zebrafish embryos that had sprouting of intersegmental blood vessels (ISV) pre-inhibited, and then tested whether the nanoparticles

could promote the recovery of ISV. As shown in Fig 4, treatment of the zebrafish embryos by VRI induced a loss of almost all their ISVs (15/16) and a majority of the head vessels (16/16) at 72 hour post fertilization (hpf). After washing the VRI and performed incubation with one of the proangiogenesis nanoparticles identified *in vitro*, ISV sprouts extended from the dorsal aorta could be easily observed (about 6 sprouts per embryos on average), and head vessels were also recovered (more than 50% of the embryos). These results indicated that these materials were capable of improving zebrafish angiogenesis *in vivo*. Consistent with the *in vitro* data, Tb Spheres was again found to be the weakest proangiogenesis nanoparticle, from which 9/19 embryos had recovered ISVs with only 3.5 sprouts per embryo.

The VRI pre-inhibition method used above was essentially the same one as previously established [18]. Under this condition, we noted that the embryos could hardly survive beyond 5 days post fertilization (dpf), although vessel-specific GFP expression was largely recovered. We tested and adopted an alternative method in which nanoparticles were added together with VRI at 24hpf and then added again without VRI at 30hpf (Fig 5 A). This new exposure scenario of VRI significantly improved the effect of nanoparticles to improve angiogenesis while inhibition of vascular structure by VRI remained complete. All embryos treated with the designated nanoparticles had their ISVs almost fully recovered and survived until 72hpf. This allowed us to determine whether the newly formed vessels were functional and supported circulation. To better visualize circulation, we used transgenic zebrafish embryos that carried both Tg(gata1:dsRed) and Tg(flk:EGFP) transgenes, which demonstrate in live embryos- the endothelial cells (green fluorescence) and circulating erythrocytes (red fluorescence) (Fig 5 B). This analysis demonstrated that the embryos treated with Eu Rods, Eu Spheres and Tb Rods had noticeable blood circulation in ISV and in the head at 72hpf. For the embryos treated with Tb Spheres, although the ISV recovered, we did not observe blood circulating in ISV, again, suggesting a weaker proangiogenesis effect.

Ionic forms of lanthanide elements enhance angiogenesis with increased angiogenesis activity in the nanoparticle form

We asked the question whether the proangiogenesis effect exerted by the materials is particle-specific. To answer that, we used europium nitrate [$Eu(NO_3)_3$] (Eu) and terbium nitrate [$Tb(NO_3)_3$] (Tb) in ionic form to compare their proangiogenesis ability with the nanoparticle forms *in vitro* and *in vivo*. As shown in Fig 6 A~B (in the zebrafish primary cell culture assay) it was evident that GFP+ cells increased after treatment with ionic Eu and Tb, *i.e.* $Eu(NO_3)_3$ and $Tb(NO_3)_3$, respectively. Quantitatively, the ionic Eu and Tb had similar ability to increase GFP+ at a cell level. These results suggested that the two ionic forms of materials that were used to synthesize the corresponding nanoparticles were capable of promoting angiogenesis *in vitro*. Similarly, as shown in Fig 6 C~E, we found the Eu and Tb in ionic form also promoted ISV sprouting *in vivo*. However, when analyzing the function of these newly formed vessels by co-incubating ionic and VRI together, none of the embryos had any circulatory vessels. This result suggested that synthesis of these lanthanide ions into nanoparticle forms increased their intrinsic ability of proangiogenesis.

H_2O_2 is necessary for the lanthanide nanoparticles to improve angiogenesis

Given the role of ROS in angiogenesis and the fact that these lanthanide nanoparticles could produce ROS, especially H_2O_2 in live tissues [7, 19], we determined if H_2O_2 was essential for proangiogenesis. This was achieved by adding catalase, a H_2O_2 scavenger, to the zebrafish embryonic primary cell culture assay and analyzing the Tg(flk:EGFP) expression. As shown in Fig 7, catalase alone slightly inhibited the GFP+ cell numbers, about a 0.8 fold compared to the blank control. When co-incubated with catalase, all of the nanoparticle treatment groups no longer were capable of promoting angiogenesis *in vitro*. This effect, we believe is specific to the nanoparticles since the catalase didn't inhibit the VEGF mediated proangiogenesis. These results suggested that the proangiogenesis action exerted by these nanoparticles were indeed mediated through the ROS pathway. Additionally, we measured mRNA level of VEGF and IL-1 by qPCR between nano-treated and untreated embryos and didn't observe significant change (Fig S3).

Materials and Methods

Lanthanide nanoparticle synthesis

Both lanthanide nanoparticles, *i.e.* $Eu^{III}(OH)_3$ and $Tb^{III}(OH)_3$, were synthesized using a hydrothermal method. In a typical synthesis of nanorods, we dissolved 1 mmoL of europium nitrate pentahydrate ($Eu(NO_3)_3 \cdot 5H_2O$) or terbium nitrate pentahydrate ($Tb(NO_3)_3 \cdot 5H_2O$) in 20 mL of deionized water in a 60 mL high-density polyethylene (HDPE) bottle. In another HDPE bottle, 10 mL of a 10 wt% potassium hydroxide (KOH, ≥85%, Sigma-Aldrich) aqueous solution was prepared. The KOH solution was then rapidly added to the lanthanide solution and the resulting mixture was vigorously mixed for 5 mins before transferring into a Teflon-lined stainless steel autoclave. All reactions were carried out in an electric oven at 200 °C for 16 hrs under autogenous pressure and static conditions. After the crystallization was complete, the autoclave was immediately cooled in a water bath. The fresh white precipitate was separated by centrifugation and washed three times with deionized water to remove ionic remnants. The final product was dried at 60 °C overnight under ambient condition. Lanthanide nanoSpheres were prepared using the same method as that for the nanorods except that an additional 2 mmoL of citric acid was added as a structure directing agent.

Transgenic zebrafish

Transgenic zebrafish line: Tg(flk:EGFP) and Tg(gata1:dsRed) were used for this study. The double-transgenic embryos were obtained by crossing homozygous Tg(flk:EGFP) and Tg(gata1:dsRed) adults. All zebrafish studies were approved by the University of California, Los Angeles Animal Care and Use Committee.

Zebrafish embryonic primary cell culture

Preparation and culture of zebrafish embryonic primary cells was described previously [17].

Imaging Capture and Analysis

The images of the 96-well plates were captured using the ImageXpress Micro XL Widefield High Content Analysis System equipped with a Nikon CCD camera. Each image taken was then analyzed using the Meta Express High Content Screening Version 5.3.0.5 software using the template Angiogenesis Tube Formation to generate data regarding tube length and branch points (Meta Express, Molecular Devices).

Microscopic imaging analysis

Cell culture plates were observed under an Axioskop 2 Plus microscope (Zeiss) at day 4, and the images were captured using an AxioCam camera and Openlab 4.0 Software (Improvision). These images were analyzed using Adobe Photoshop CS6 by creating a new transparent layer to cover the original layer in each image. In this new layer, the GFP+ cells were traced to reveal outlines on the original cell images. The pixel value of the transparent layer was used to define the level of endothelial cell differentiation.

Zebrafish angiogenesis inhibited model

Transgenic zebrafish embryos were cleaned and grown in 24-well plates at 28 °C. Each well contained 500 μL of Holtfreter's solution and 20 embryos. A final concentration of 450 nM VEGFR tyrosine kinase inhibitor II (VRI) was added in each well at 24 hpf and washed out at 30 hpf. The exposure of the nanoparticles was initiated by adding 100 μg/ml of the suspension into each well of the 24-well plate. These embryos were placed on a shaker at a speed of 120 rpm which prevented the particles to aggregate. At 72hpf, the embryos were observed under an Axioskop 2 Plus microscope (Zeiss). Embryos were imaged using an AxioCam camera and analyzed using Openlab 4.0 Software (Improvision).

An initial co-incubation method was designed to study zebrafish circulation function. Instead of first adding VRI at 24 hpf and then adding nanoparticles at 30 hpf, embryos were co-exposed with 100 μg/ml nanoparticles and 450 nM VRI starting at 24 hpf and the mixed solution was replaced by Holtfreter's solution, containing 100 μg/ml nanoparticles, after washing out the initial mix.

Discussion

Angiogenesis is a complex process of forming blood vessels from existing vessels. In animals, angiogenesis is critically involved in various biology processes, such as embryonic development, tissue repair and wound healing [3, 20, 21]. The identification of new types of pro-angiogenesis materials will benefit the development of regenerative medicine. Use of nanomaterials for this purpose is a relatively new concept. Nanoparticles can be synthesized in many different compositions, sizes, and shapes. Further modification of candidates with proangiogenesis activity could lead to nanoproducts with improved characteristics that are safer for clinical application. The approach we employed here should be very useful to analyze large numbers of nanoparticles in a relatively short time frame. In addition of being a good model for studying developmental biology and human diseases, the study presented here establishes that zebrafish can also be an excellent high throughput animal system for

screening biologically active agents for research and therapeutic purposes [22–24] in an effective manner.

We identified spherical and rod-shape nanoparticles of $Eu^{III}(OH)_3$ and $Tb^{III}(OH)_3$ as candidates for enhancing angiogenesis. All of them significantly promoted angiogenesis in our *in vitro* and *in vivo* model. In order to demonstrate this functionality, *i.e.* blood circulation, we developed and adopted a new method (Fig 4 A). Using this method, one can differentiate particles that enhance the growth of endothelial cells and the reestablishment of circulation. All the 4 nanoparticles we tested promoted angiogenesis and induced the recovery vessels to form a complete ISV system, albeit the Tb Spheres treated embryos still lacked blood flow. In our case, the concentrations at which nanoparticles worked best to promote angiogenesis were at 1 μg/ml *in vitro*, and 100 μg/ml *in vivo*. It requires higher concentrations to have effect *in vivo* on whole embryos because nanoparticles need to act on the surface of the body and induce angiogenesis that occurs inside of the body. When we used a concentration higher than 1 and 100 μg/ml, respectively, we observed toxicity.

Up until now, it has not been fully investigated whether the proagiogenesis activity of nanoparticles ([7]) stems from the different shaped lanthanide nanoparticles or the original element itself in its ionic form. In this study, we showed that the ability of promoting angiogenesis is likely a result of both. Ionic forms of Eu and Tb were both capable of enhancing angiogenesis. However, this effect was further enhanced when they are synthesized in nanoparticle form. We noted that Tb rods are more effective than Tb spheres. However, it remains to be investigated how the specific size and shape of Eu and Tb or other types of nanoparticles affect angiogenesis.

The enhancement of proangiogenesis activity by synthesizing different forms of nanoparticles is likely due to production of ROS, which is specific to nano structures. ROS are a series of small chemically reactive molecules, which increase oxidative stress in cells and tissue. Although considered as a byproduct of metabolism, ROS regulates angiogenesis through reversible oxidase with some key signaling components that has been demonstrated in the last decade [10, 11]. Similar to our findings, several other nanoparticles, such as cerium nanorods, copper sulfide nanocrystals and silver nanoparticles also have been shown to promote angiogenesis or generate ROS [25–29]. Most of these studies were carried out using HUVEC and chicken embryo chorioallantoic membrane (CAM) as *in vitro* and *in vivo* assays, which are not easily scalable. We use transgenic zebrafish expressing vascular GFP as a single organism to offer both *in vitro* and *in vivo* assays that should be amendable to high throughput screening. Consistent with previous findings, we demonstrate that Eu and Tb nanoparticles could also generate ROS and provide a proangiogenesis effect *in vivo* and *in vitro*. In particular, H_2O_2 is the key factor of the proangiogenesis effect found in these nanoparticles. This was revealed by loss of proangiogenesis activity after adding catalase, which removes H_2O_2 by converting it to water and oxygen [30]. This is specific to nanoparticles because catalase did not inhibit proangiogenesis activity of VEGF under the same condition.

In summary, we developed high throughput screening systems to evaluate proangiogenesis candidates. Based on these systems, we found that lanthanide nanoparticles, both rod and sphere shape, promote angiogenesis through H_2O_2, sensitive signaling.

Supplementary Material

Refer to Web version on PubMed Central for supplementary material.

References

1. Novakova V, Sandhu GS, Dragomir-Daescu D, Klabusay M. Vascul Pharmacol. 2015
2. Rosano GM, Fini M, Caminiti G, Barbaro G. Curr Pharm Des. 2008; 14(25):2551–2562. [PubMed: 18991672]
3. Stoekenbroek RM, Boekholdt SM, Fayyad R, Laskey R, Tikkanen MJ, Pedersen TR, Hovingh GK. Incremental Decrease in End Points Through Aggressive Lipid Lowering Study, G. Heart. 2015; 101(5):356–362. [PubMed: 25595417]
4. Flammer AJ, Anderson T, Celermajer DS, Creager MA, Deanfield J, Ganz P, Hamburg NM, Luscher TF, Shechter M, Taddei S, Vita JA, Lerman A. Circulation. 2012; 126(6):753–767. [PubMed: 22869857]
5. van Mil A, Grundmann S, Goumans MJ, Lei Z, Oerlemans MI, Jaksani S, Doevendans PA, Sluijter JP. Cardiovasc Res. 2012; 93(4):655–665. [PubMed: 22227154]
6. Patra CR, Bhattacharya R, Patra S, Vlahakis NE, Gabashvili A, Koltypin Y, Gedanken A, Mukherjee P, Mukhopadhyay D. Advanced Materials. 2008; 20(4):753–756.
7. Patra CR, Kim JH, Pramanik K, d'Uscio LV, Patra S, Pal K, Ramchandran R, Strano MS, Mukhopadhyay D. Nano Lett. 2011; 11(11):4932–4938. [PubMed: 21967244]
8. Kamata H, Hirata H. Cell Signal. 1999; 11(1):1–14. [PubMed: 10206339]
9. Devasagayam TP, Tilak JC, Boloor KK, Sane KS, Ghaskadbi SS, Lele RD. J Assoc Physicians India. 2004; 52:794–804. [PubMed: 15909857]
10. Kajla S, Mondol AS, Nagasawa A, Zhang Y, Kato M, Matsuno K, Yabe-Nishimura C, Kamata T. FASEB J. 2012; 26(5):2049–2059. [PubMed: 22278940]
11. Chatterjee S, Fisher AB. Antioxid Redox Signal. 2014; 20(6):899–913. [PubMed: 24328670]
12. Zhang M, Brewer AC, Schroder K, Santos CX, Grieve DJ, Wang M, Anilkumar N, Yu B, Dong X, Walker SJ, Brandes RP, Shah AM. Proc Natl Acad Sci U S A. 2010; 107(42):18121–18126. [PubMed: 20921387]
13. Page EL, Chan DA, Giaccia AJ, Levine M, Richard DE. Mol Biol Cell. 2008; 19(1):86–94. [PubMed: 17942596]
14. Xia C, Meng Q, Liu LZ, Rojanasakul Y, Wang XR, Jiang BH. Cancer Res. 2007; 67(22):10823–10830. [PubMed: 18006827]
15. Haddad P, Dussault S, Groleau J, Turgeon J, Maingrette F, Rivard A. Atherosclerosis. 2011; 217(2):340–349. [PubMed: 21524749]
16. Ostman A, Frijhoff J, Sandin A, Bohmer FD. J Biochem. 2011; 150(4):345–356. [PubMed: 21856739]
17. Huang H, Lindgren A, Wu X, Liu NA, Lin S. Cell Rep. 2012; 2(3):695–704. [PubMed: 22999940]
18. Li S, Dang YY, Oi Lam Che G, Kwan YW, Chan SW, Leung GP, Lee SM, Hoi MP. Toxicol Appl Pharmacol. 2014; 280(3):408–420. [PubMed: 25234792]
19. Sies H. Exp Physiol. 1997; 82(2):291–295. [PubMed: 9129943]
20. Mitsos S, Katsanos K, Koletsis E, Kagadis GC, Anastasiou N, Diamantopoulos A, Karnabatidis D, Dougenis D. Angiogenesis. 2012; 15(1):1–22. [PubMed: 22120824]
21. Majewska I, Gendaszewska-Darmach E. Acta Biochim Pol. 2011; 58(4):449–460. [PubMed: 22030557]
22. Patton EE, Zon LI. Nature reviews. Genetics. 2001; 2(12):956–966.

23. McAleer MF, Davidson C, Davidson WR, Yentzer B, Farber SA, Rodeck U, Dicker AP. Int J Radiat Oncol Biol Phys. 2005; 61(1):10–13. [PubMed: 15629588]
24. Lally BE, Geiger GA, Kridel S, Arcury-Quandt AE, Robbins ME, Kock ND, Wheeler K, Peddi P, Georgakilas A, Kao GD, Koumenis C. Cancer Res. 2007; 67(18):8791–8799. [PubMed: 17875720]
25. Das S, Singh S, Dowding JM, Oommen S, Kumar A, Sayle TX, Saraf S, Patra CR, Vlahakis NE, Sayle DC, Self WT, Seal S. Biomaterials. 2012; 33(31):7746–7755. [PubMed: 22858004]
26. Kang K, Lim DH, Choi IH, Kang T, Lee K, Moon EY, Yang Y, Lee MS, Lim JS. Toxicol Lett. 2011; 205(3):227–234. [PubMed: 21729742]
27. Mroczek-Sosnowska N, Sawosz E, Vadalasetty KP, Lukasiewicz M, Niemiec J, Wierzbicki M, Kutwin M, Jaworski S, Chwalibog A. Int J Mol Sci. 2015; 16(3):4838–4849. [PubMed: 25741768]
28. Liu Z, Liu X, Du Y, Ren J, Qu X. ACS Nano. 2015; 9(10):10335–10346. [PubMed: 26331394]
29. Guan Y, Li M, Dong K, Ren J, Qu X. Small. 2014; 10(18):3655–3661. [PubMed: 24839962]
30. Cong W, Ruan D, Xuan Y, Niu C, Tao Y, Wang Y, Zhan K, Cai L, Jin L, Tan Y. J Mol Cell Cardiol. 2015

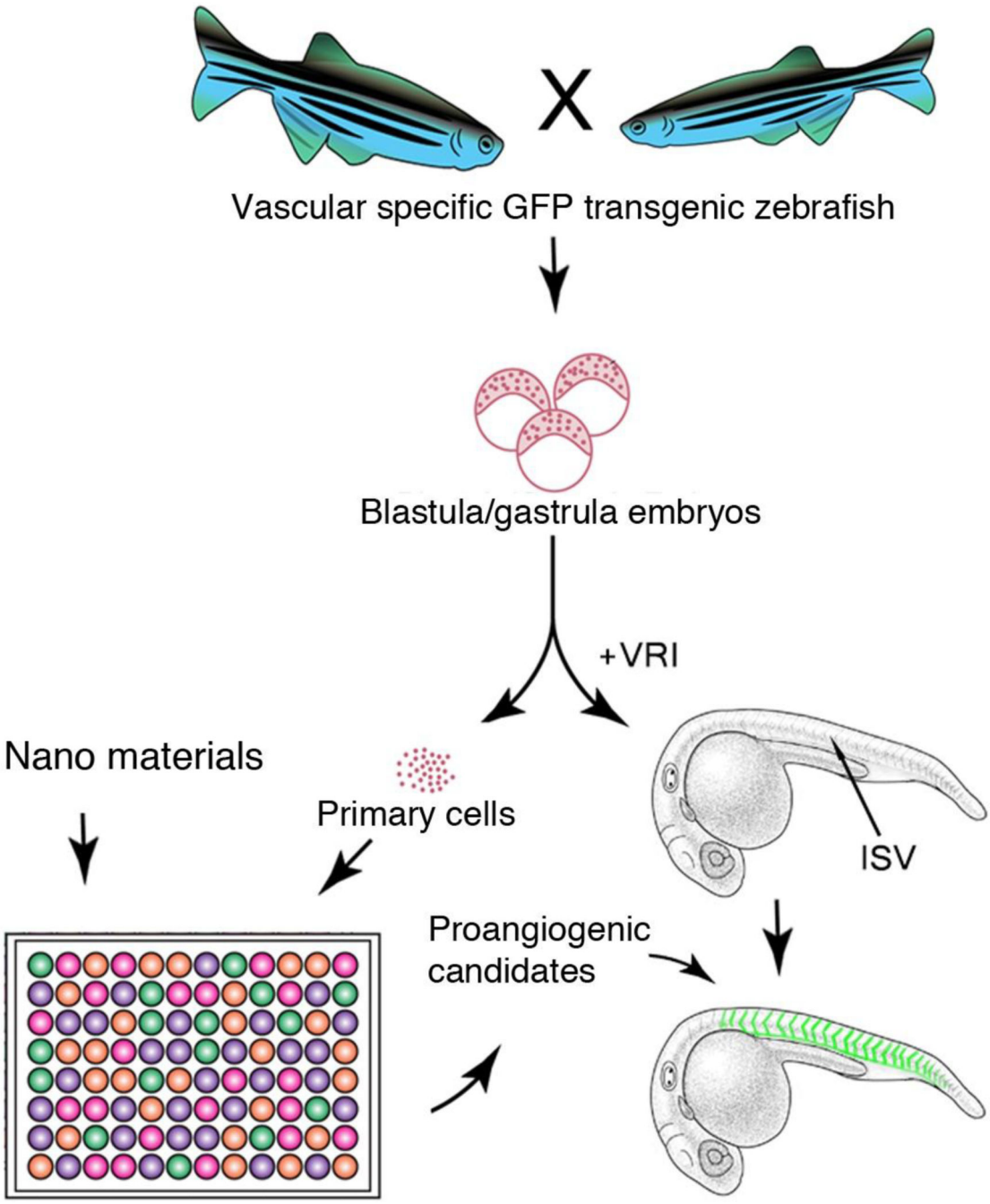

Figure 1.

Schematic diagram showing the overall strategy and methodology of our experiments illustrating Tg(flk:EGFP) transgenic primary cell and whole embryo based high throughput screening for nanomaterials with proangiogenesis activity.

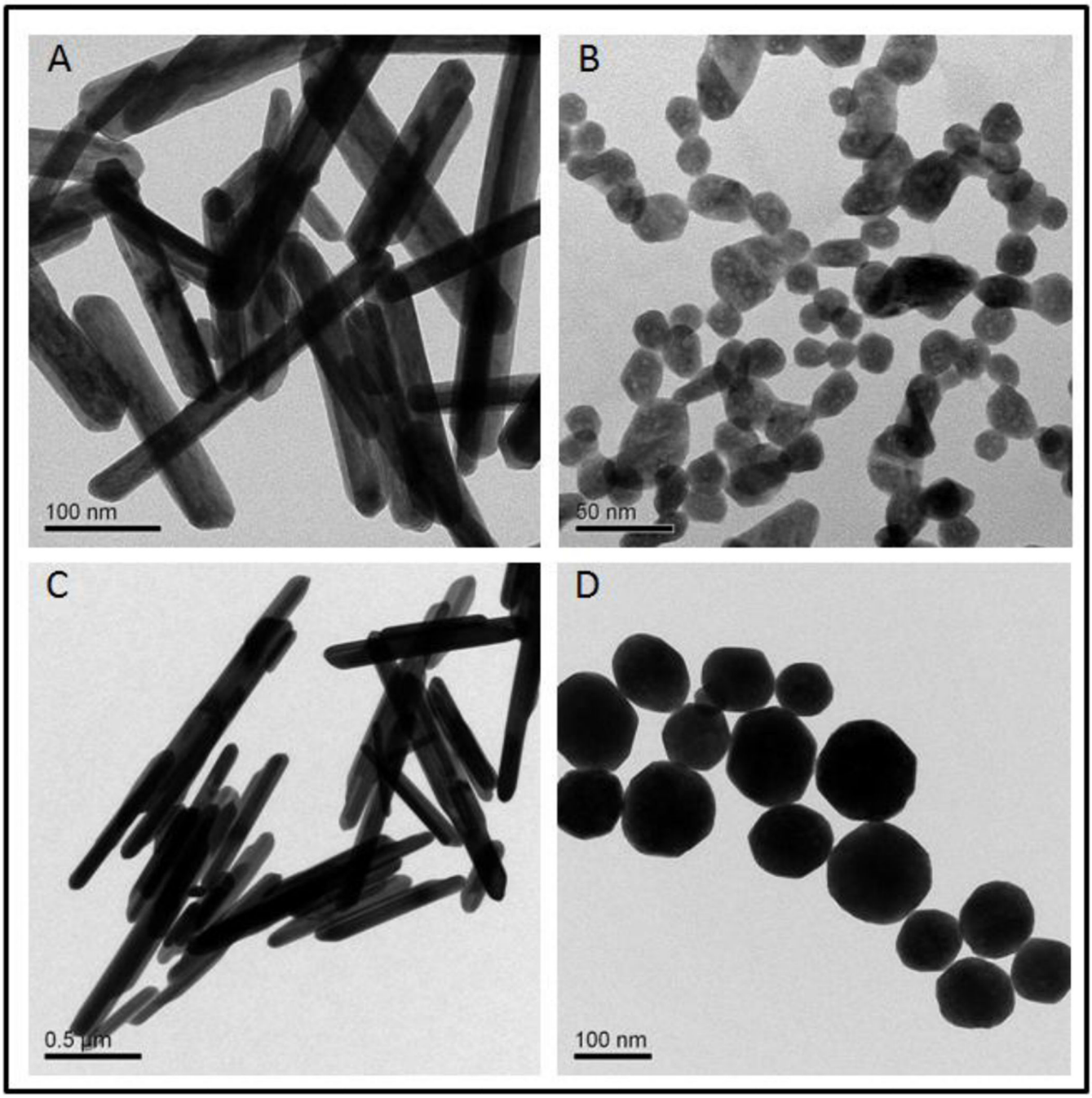

Figure 2.

Representative TEM images of nanoparticles with proangiogenesis activity. **A.** Eu Rods. **B.** Eu Spheres. **C.** Tb Rods. **D.** Tb Spheres.

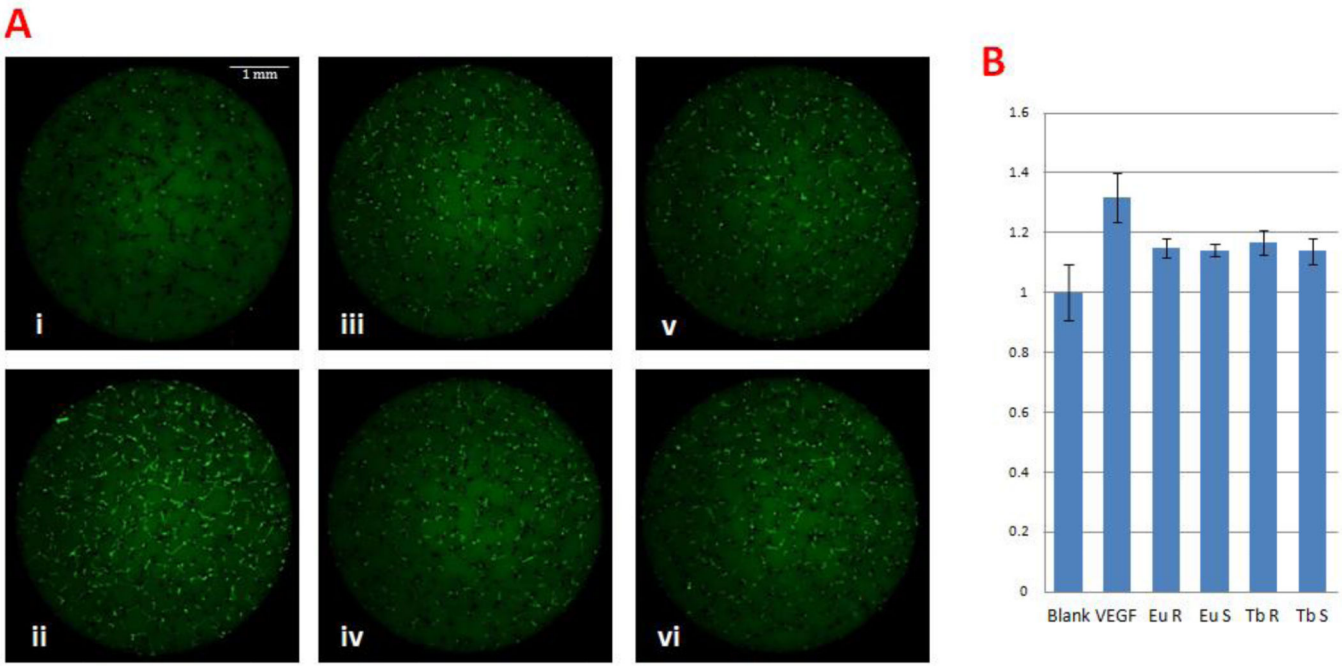

Figure 3.

Lanthanide nanoparticles induced angiogenesis *in vitro*. **A.** Embryonic primary cell culture with 1μg/ml nanoparticles or 20 ng/ml VEGF. i) Blank control, ii) 20 ng/ml VEGF, iii) 1 μg/ml Eu Rods, iv) 1 μg/ml Eu Spheres, v) 1 μg/ml Tb Rods, vi) 1 μg/ml Tb Spheres. VEGF exerted significantly improved GFP+ cell proliferation. Nanoparticles also show proangiogenesis ability. **B.** Quantitative analysis by Meta Express High Content Screening software.

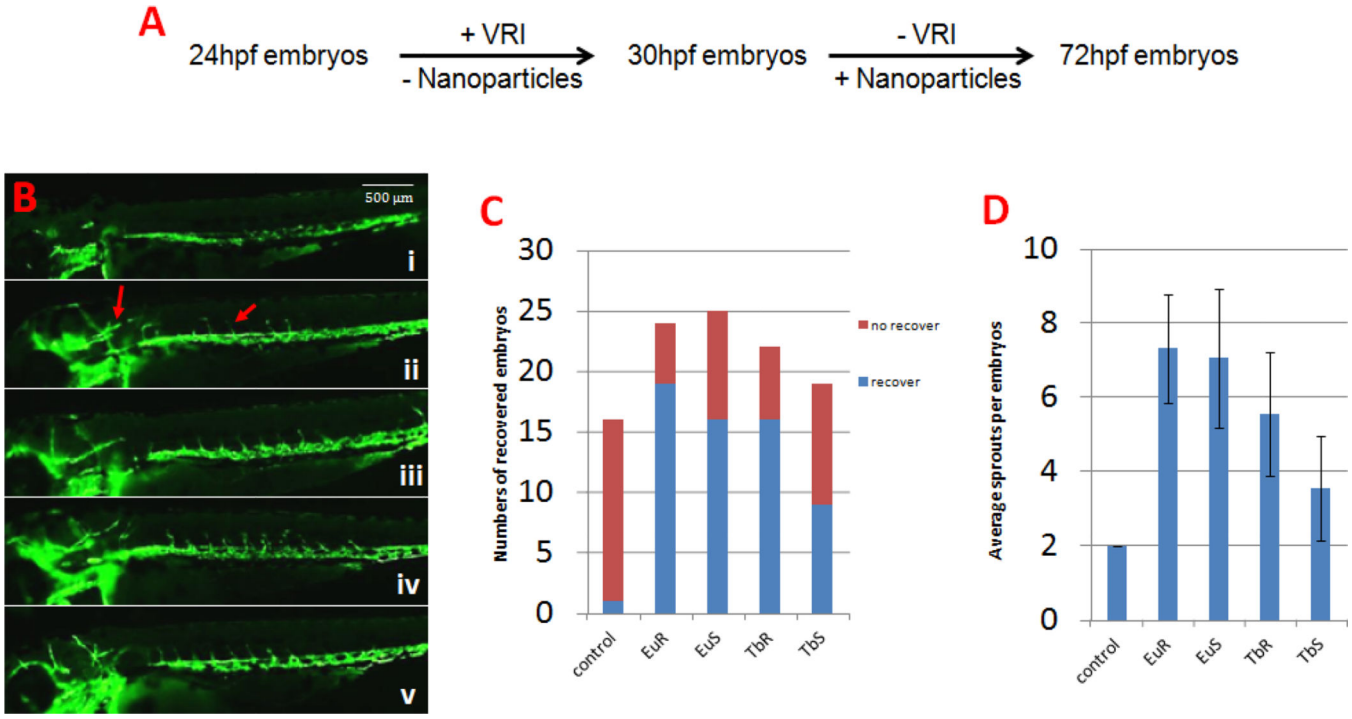

Figure 4.

Lanthanide nanoparticles could improve angiogenesis *in vivo*. **A**. The methodology of VRI induced zebrafish angiogenesis deficiency model. **B.** Zebrafish embryos at 72 hpf. i) Blank control, ii) 100 μg/ml Eu Rods, iii) 100 μg/ml Eu Spheres, iv) 100 μg/ml Tb Rods, v) 100 μg/ml Tb Spheres. Compared with blank control, vessel sprouts can be found in ISV region and head under nanoparticle treatment. **C.** Graph to show the numbers of ISV recovered embryos. **D.** Graph to show average ISV sprouts per embryo. The ISV sprouts increased at different levels after nanoparticle treatment.

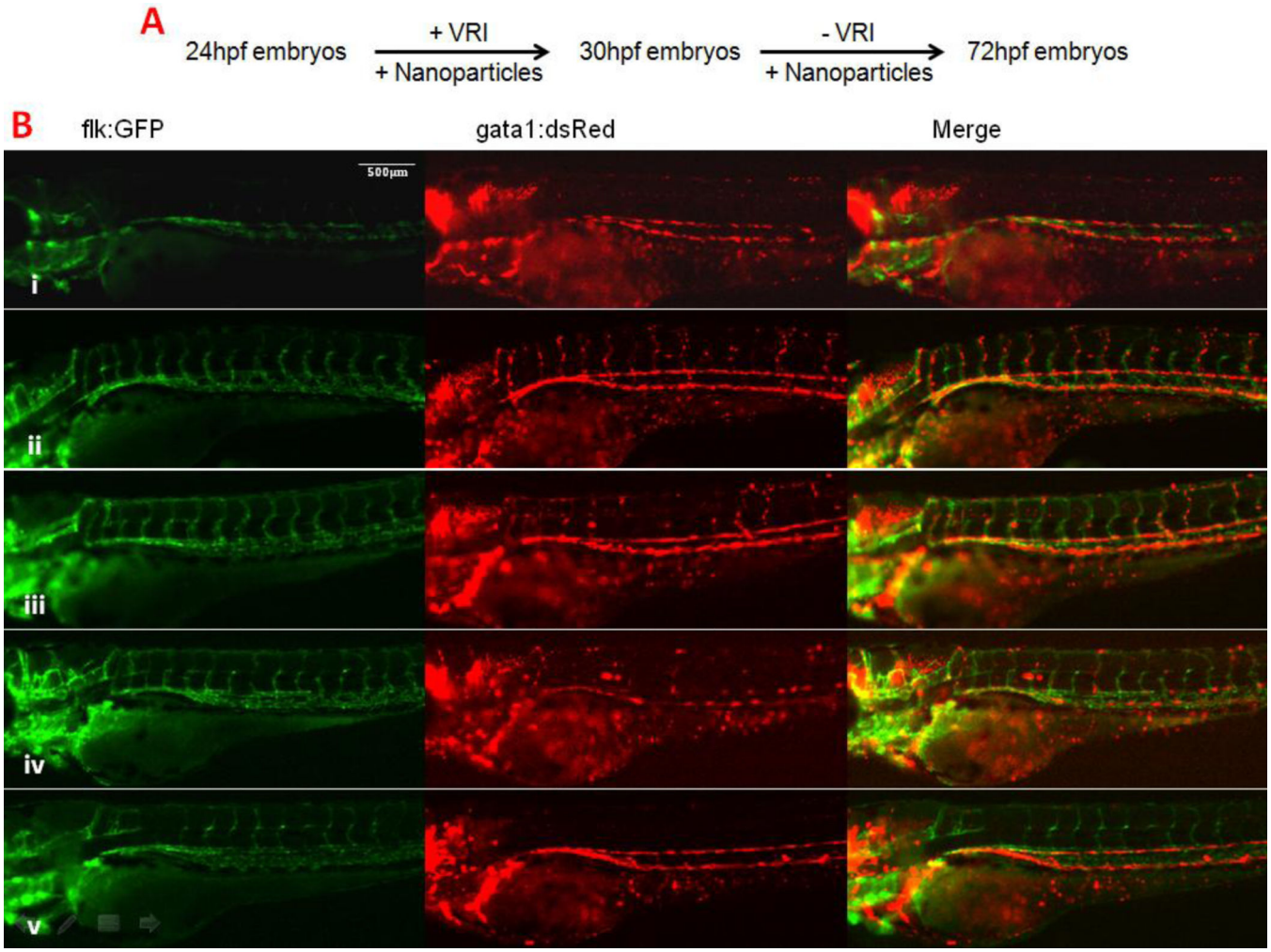

Figure 5.

Lanthanide nanoparticles could recover circulation in VRI pre-treated zebrafish embryos. **A.** Alternative method for studying the function of recovered ISV vessel. **B.** Zebrafish embryos at 72 hpf. i) Blank control, ii) 100 μg/ml Eu Rods, iii) 100 μg/ml Eu Spheres, iv) 100 μg/ml Tb Rods, v) 100 μg/ml Tb Spheres. The green channel represents the blood vessels, while the red channel represents the mature blood cells. The merged pictures indicate that the embryonic circulation in the ISV region has recovered after treatment of nanoparticles in this method (also see supplementary movies).

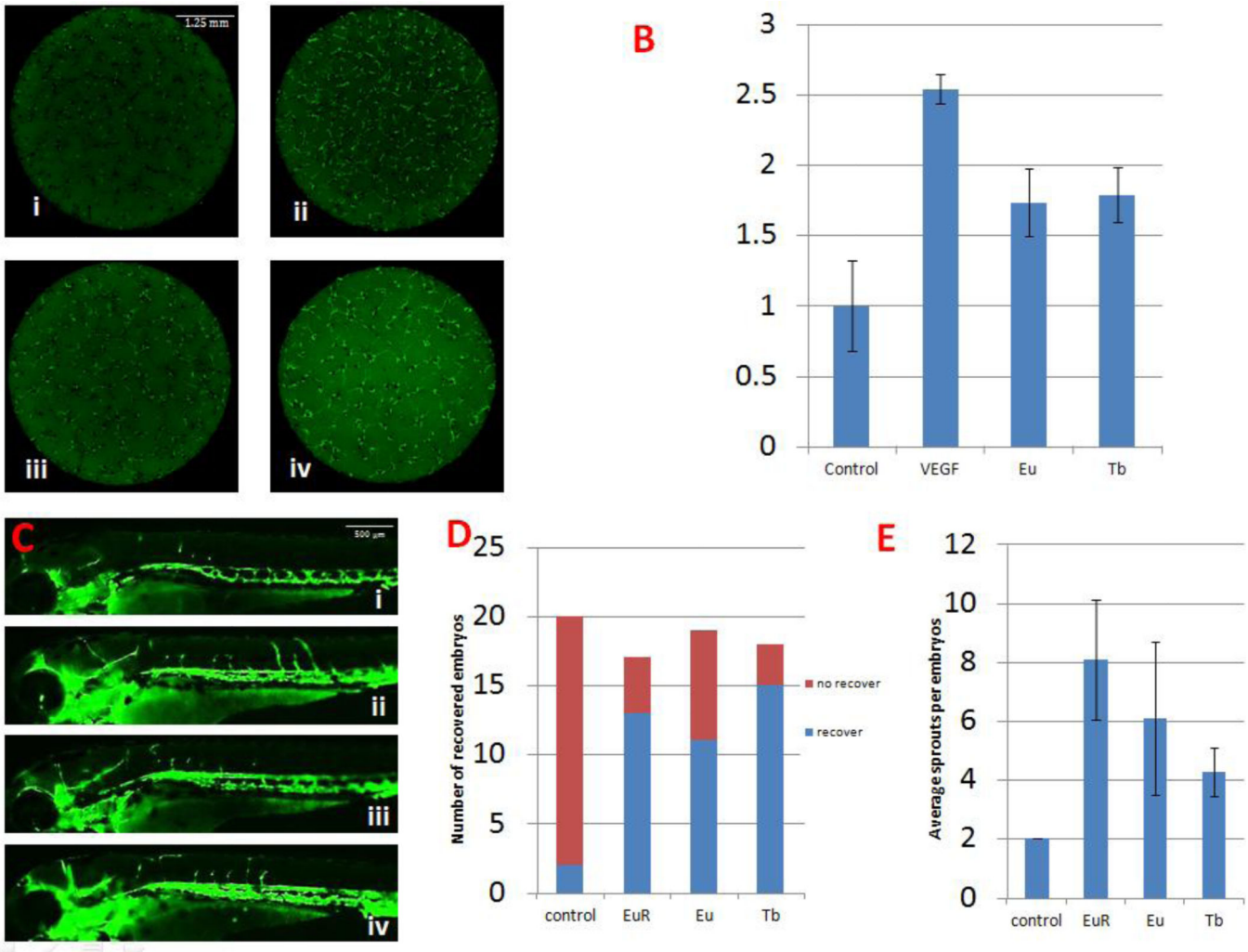

Figure 6.

Both ionic forms of europium and terbium show proangiogenesis effect *in vitro* and *in vivo*. **A.** Primary cell culture with 1 μg/ml Eu or Tb. i) Blank control, ii) 20 ng/ml VEGF, iii) 1 μg/ml Eu, iv) 1 μg/ml Tb. **B.** Compared with blank control, an increase of GFP+ cells can be observed after Eu or Tb treatment. **C.** Zebrafish embryos at 72 hpf. i) Blank control, ii) 100 μg/ml Eu Rods, iii) 100 μg/ml Eu, iv) 100 μg/ml Tb. The recovering ISV shows the proangiogenesis ability of ionic forms of europium and terbium. **D.** Graph to show number of ISV recovered embryos. **E.** Graph to show average ISV sprouts per embryo.

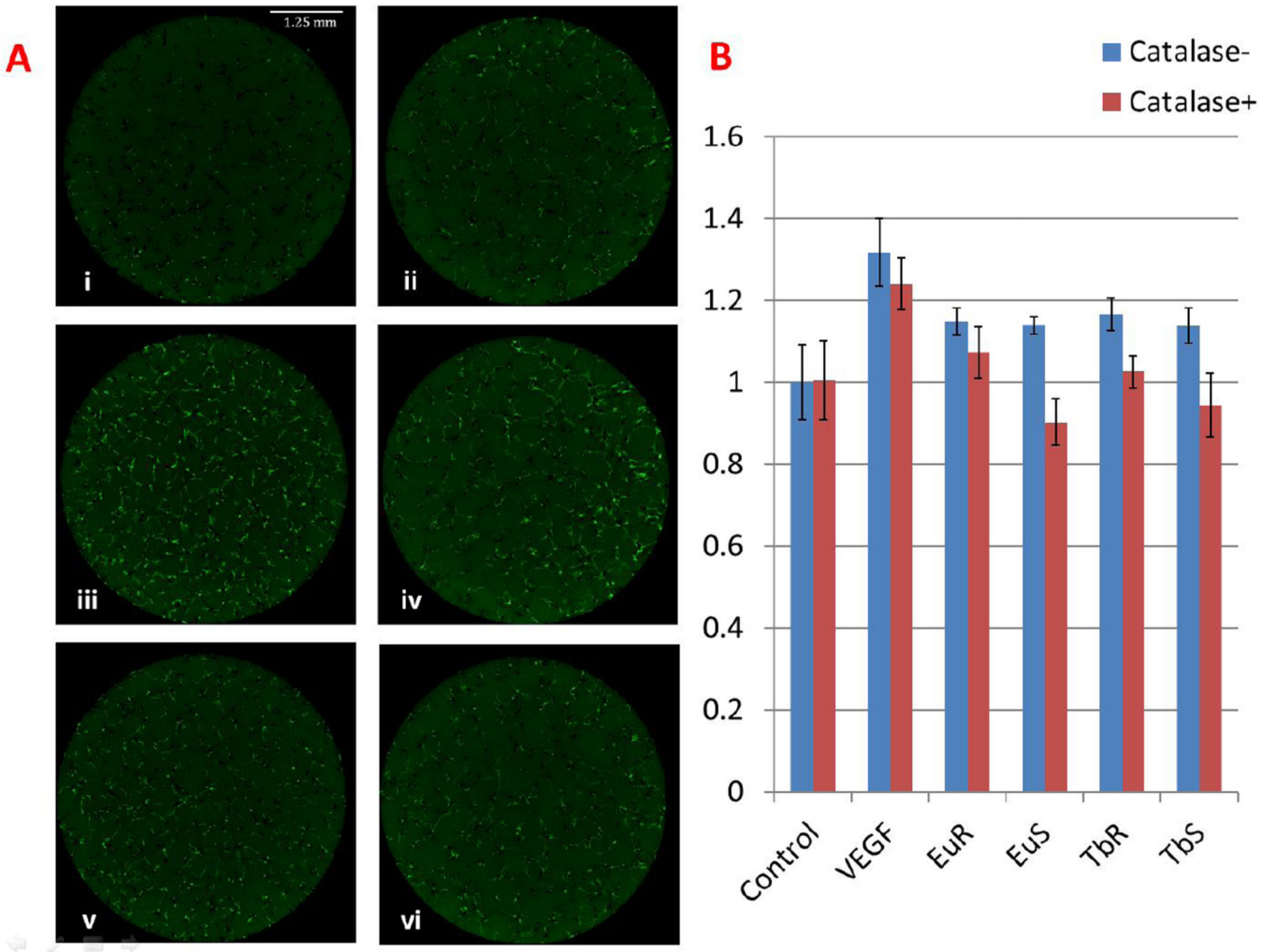

Figure 7.

H_2O_2 is necessary for nanoparticles proangiogenesis activity. **A.** Primary cell culture with 1 μg/ml nanoparticles and 1000 units/ml catalase. i) Blank control, ii) 1000 units/ml catalase, iii) 20 ng/ml VEGF, iv) 20 ng/ml VEGF and 1000 units/ml catalase, v) 1 μg/ml Eu Rods, vi) 1 μg/ml Eu Rods and 1000 units/ml catalase. **B.** Quantitative analysis shows that catalase can abolish proangiogenesis activity induced by nanoparticles, but not by VEGF.